Phylogenetic diversity and functional analysis of metal transporters of the Cation Diffusion Facilitator family from algae

Aniefon Ibuot [a], Andrew P. Dean [b], and Jon K. Pittman [c,*]

[a] Department of Science Technology, Akwa Ibom State Polytechnic, Ikot Osurua, P.M.B 1200.Ikot Ekpene, Akwa Ibom State, Nigeria

[b] Department of Natural Sciences, Faculty of Science and Engineering, Manchester Metropolitan University, Oxford Road, Manchester, M1 5GD, UK

[c] Department of Earth and Environmental Sciences, School of Natural Sciences, Faculty of Science and Engineering, The University of Manchester, Michael Smith Building, Oxford Road, Manchester M13 9PT, UK

*Corresponding Author:

Dr Jon Pittman, Department of Earth and Environmental Sciences, The University of Manchester, Michael Smith Building, Oxford Road, Manchester M13 9PT, UK; Tel: +44 (0)161 275 5235; Fax: +44 (0)161 275 5082; Email: jon.pittman@manchester.ac.uk

Orchid ID: 0000-0001-7197-1494

1

Abstract

Metal transport processes are relatively poorly understood in algae in comparison to higher plants and other eukaryotes. A screen of genomes from 33 taxonomically diverse algal species was conducted to identify members of the Cation Diffusion Facilitator (CDF) family of metal ion transporter. All algal genomes contained at least one CDF gene, further confirming that this is a ubiquitous gene family. Phylogenetic analysis suggested a CDF gene organisation of five groups, which includes Zn-CDF, Fe/Zn-CDF and Mn-CDF groups, consistent with previous phylogenetic analyses, and two undefined groups. One of these undefined groups was algal specific although excluded chlorophyte and rhodophyte sequences. Sequences from this group had a putative ion binding site motif that was distinct from other CDF proteins. The phylogenetic grouping was supported by sequence cluster analysis. Yeast heterologous expression of CDF proteins from *Chlamydomonas reinhardtii* indicated Zn^{2+}, Co^{2+} and/or Mn^{2+} transport function by the different isoforms, which validated the phylogenetic prediction, although one member of the Mn-CDF group was also able to provide Zn tolerance to yeast. There is wide diversity of CDF transporters within the algae lineage, and some of these genes may be attractive targets for future applications of metal content engineering in plants or microorganisms.

Keywords: algae phylogenetics, *Chlamydomonas reinhardtii*, manganese transport, metal tolerance, yeast heterologous expression, zinc transport

Introduction

Knowledge of the transport pathways for metal influx, efflux and subcellular metal partitioning in plant and algal cells is critical in order to understand the processes of essential metal homeostasis within the cell. These will include pathways for essential trace metals such as zinc, copper and manganese, which are required for many biochemical functions including as enzyme co-factors or structural components of proteins (Andreini et al. 2008). Furthermore, both essential and non-essential metals, such as cadmium, are toxic at elevated concentrations and so transporters play a key role in protecting the cell against metal toxicity (Kramer et al. 2007). This protection can be mediated by metal efflux from the cell or intracellular metal sequestration into compartments such as the vacuole (Sharma et al. 2016). Manipulation of expression of specific transporter proteins, such as by genetic engineering, can therefore be used to enhance metal tolerance of an organism (Antosiewicz et al. 2014). Moreover, manipulation of metal sequestration may also provide increased total metal content within a cell whilst still providing metal tolerance, and would be useful for metal bioremediation applications (Ibuot et al. 2017; Cheng et al. 2019).

Microalgae are one such group of organisms that have been proposed as potentially suitable for metal bioremediation (Suresh Kumar et al. 2015), but if genetic engineering of metal transporters is to be tested in microalgae then molecular targets that have been functionally characterised are needed. Genomic analyses of green microalgae, such as *Chlamydomonas reinhardtii*, and red microalgae, such as *Cyanidioschyzon merolae* indicate that there are a wide variety of metal transporter pathways that are conserved between microalgae and higher plants alongside other eukaryotes such as yeast (Hanikenne et al. 2005; Blaby-Haas and Merchant 2012). One such metal transporter family is the Cation Diffusion Facilitator (CDF) family, which are referred to as Metal Transport Proteins (MTP) in higher plants (Ricachenevsky et al. 2013; Kolaj-Robin et al. 2015). CDF-type transporters have been reported to facilitate the transport of metals including Cd^{2+}, Co^{2+}, Cu^{2+} Fe^{2+}, Mn^{2+}, Ni^{2+}, and Zn^{2+}, and are found virtually in all organisms covering the Eukaryote, Eubacteria and Archaea kingdoms (Nies and Silver 1995; Cubillas et al. 2013). In yeast and plants,

3

CDF/MTP proteins localise to membranes of various intracellular compartments, in particular the vacuolar membrane but also the mitochondria, endoplasmic reticulum (ER), Golgi/trans-Golgi and pre-vacuolar compartment, where they are involved in the efflux of metals from the cytoplasm into these organelles (Haney et al. 2005; Ricachenevsky et al. 2013). For example, in *Saccharomyces cerevisiae*, CDF proteins mediate Zn^{2+} and Co^{2+} transfer into the vacuole (ScZrc1 and ScCot1), Zn^{2+} transfer into the ER (ScZrg17 and ScMsc2) and Fe^{2+} transfer from the mitochondria (ScMmt1 and ScMmt2) (MacDiarmid et al. 2002; Ellis et al. 2005; Li et al. 2014). In *Arabidopsis thaliana*, AtMTP1 and related orthologues including AtMTP3 play a major role in the storage and sequestration of Zn^{2+} in the vacuole (Kobae et al. 2004; Arrivault et al. 2006), AtMTP5 and AtMTP12 transport Zn^{2+} into the Golgi (Fujiwara et al. 2015), while AtMTP8 and AtMTP11 mediate Mn^{2+} transport into the vacuole and Golgi (Delhaize et al. 2007; Peiter et al. 2007; Eroglu et al. 2016).

The current understanding of CDF/MTP proteins in algae is limited. The CDF gene family appears to be present in all previously examined algal species (Gustin et al. 2011; Blaby-Haas and Merchant 2012, 2017) but specific details about CDF family structures within individual species are unknown. Phylogenetic analysis will be able to reveal some useful details since substrate specificity seems to be related to phylogeny (Montanini et al. 2007; Cubillas et al. 2013). Within the well-studied model microalga *C. reinhardtii* there are five putative MTP genes (CrMTP1 to CrMTP5). Some of these genes are transcriptionally induced by Zn or Mn deficiency conditions (Allen et al. 2007; Malasarn et al. 2013) but to date only CrMTP4 has been functionally characterised as a Mn^{2+} and Cd^{2+} transporter (Ibuot et al. 2017). This was determined by performing over-expression of CrMTP4 in *C. reinhardtii* yielding enhanced Cd tolerance, and by using yeast (*S. cerevisiae*) heterologous expression where CrMTP4 was able to rescue the Mn sensitive phenotype of the *pmr1* yeast mutant. In this study, we aimed to perform a large-scale phylogenetic analysis of putative MTP genes from available algal genome sequences in order to evaluate the potential diversity within this broad taxonomic lineage. Furthermore, a characterisation of additional members of the *C.*

4

reinhardtii MTP gene family was carried out by using yeast heterologous expression to infer the metal substrates and determine metal tolerance functions.

Materials and methods

Bioinformatic analysis

Thirty three algal species genomes were screened from 1 Charophyta: *Klebsormidium nitens*; 13 Chlorophyta: *Bathycoccus prasinos* RCC1105, *Botryococcus braunii*, *Chlamydomonas reinhardtii*, *Chlorella* sp. NC64A, *Chromochloris zofingiensis*, *Coccomyxa subellipsoidea* C-169, *Dunaliella salina*, *Micromonas pusilla* CCMP1545, *Micromonas* sp. RCC299, *Ostreococcus lucimarinus*, *Ostreococcus* sp. RCC809, *Ostreococcus tauri* RCC4221, *Volvox carteri*; 2 Pelagophyta: *Aureococcus anophagefferens* clone 1984, *Pelagophyceae* sp. CCMP2097; 2 Cryptophyta: *Cryptophyceae* sp. CCMP2293, *Guillardia theta* CCMP2712; 3 Rhodophyta: *Cyanidioschyzon merolae*, *Galdieria sulphuraria* 074W, *Porphyra umbilicalis*; 4 Haptophyta: *Emiliania huxleyi* CCMP1516, *Pavlovales* sp. CCMP2436, *Phaeocystis antarctica* CCMP1374, *Phaeocystis globosa* Pg-G; 4 Bacillariophyta: *Fragilariopsis cylindrus* CCMP 1102, *Phaeodactylum tricornutum* CCAP 1055/1, *Pseudo-nitzschia* multiseries CLN-47, *Thalassiosira pseudonana* CCMP 1335; 3 Ochrophyta: *Ectocarpus siliculosus* Ec 32, *Nannochloropsis oceanica* CCMP1779, *Ochromonadaceae* sp. CCMP2298; and 1 Chlorarachniophyta: *Bigelowiella natans* CCMP2755. In addition, other species genomes were screened for comparison from the cyanobacterium *Nostoc punctiforme* PCC 73102, human *Homo sapiens*, land plant *Arabidopsis thaliana*, yeast *Saccharomyces cerevisiae*, and the thraustochytrid *Schizochytrium aggregatum* ATCC 28209. Finally sequences from ten bacteria and one archeae were used. Genome details and individual ID numbers or accession numbers for the sequences used are provided in Supplementary Information and in Supplementary Table S1.

Genomes were screened by BLAST using *C. reinhardtii* and *S. cerevisiae* CDF protein sequences. In addition, genomes were screened for the presence of the Pfam

domain PF01545. All sequences were then manually examined by sequence alignment to remove any false positive sequences that had been mis-annotated. Amino acid multiple sequence alignments were performed using Clustal Omega (Madeira et al. 2019). For visual analysis sequence alignments were shaded using BoxShade v.3.21 and manually annotated. Prediction of transmembrane domains (TMD) was performed by hydropathy analysis using TMHMM v.2.0 (Krogh et al. 2001) and was performed by consensus topology prediction using TOPCONS (Tsirigos et al. 2015). His-rich loop presence was determined by manual analysis by identifying the presence of three or more histidine residues within the putative cytosolic loop region between TMD 4 and 5. Conserved residues within TMD2 and TMD5 of Group 1 (Zn-CDF) and Group 5 sequences were identified using WebLogo v.2.8.2 (Crooks et al. 2004).

Phylogenetic relationships at the amino acid level were performed using full length sequences, essentially as described previously (Emery et al. 2012; Pittman and Hirschi 2016). Sequence alignment outputs from Clustal Omega were used to generate maximum likelihood phylogenies under the WAG+F model of amino acid substitution with Γ-distributed rates across sites, as implemented in RAxML v7.1, with tree confidence determined from 1000 replications using the fast bootstrap method (Stamatakis 2006; Stamatakis et al. 2008). The trees were viewed using FigTree v1.3 (http://tree.bio.ed.ac.uk/software/figtree).

The relationship between sequences was further quantified using Cluster Analysis of Sequences (CLANS) (Frickey and Lupas 2004), which was used to conduct an all-against-all BLAST of unaligned sequences. Pairwise similarities between protein sequences were displayed in a 2-dimensional cluster plot using CLANS Jar from the MPI Bioinformatics Toolkit (Zimmermann et al. 2018). The P value was set to 1×10^{-5} and the analysis was run for 50,000 iterations.

Microalgae cultivation and RNA isolation

C. reinhardtii (CC125) was obtained from the Chlamydomonas Resource Center, USA, and was grown photo-heterotrophically in batch culture in Tris–acetate–phosphate (TAP)

6

medium at pH 7 (Harris 1989) in 200 mL glass flasks on an orbital shaker rotating at 2 Hz, at

25°C under cool-white fluorescent lights (150 μmol m^{-2} s^{-1}) with a 16-h:8-h light:dark regime.

Cultures were inoculated with the same starting cell density as determined by cell counting

to give an initial cell count of ~65 x 10^3 cells ml^{-1}. RNA was isolated from exponential

growing *C. reinhardtii* CC125 cells using Trizol reagent (Life Technologies) and further

purified by phenol/chloroform extraction and precipitation with isopropanol.

MTP full length cDNA cloning

C. reinhardtii genomic sequence and gene model information was obtained from Phytozome

v.9.1 using v.5.3 of the *C. reinhardtii* genome annotations and gene-specific oligonucleotide

primers incorporating restriction enzyme sites (Supplementary Table S2) were designed to

amplify the full-length *CrMTP1*, *CrMTP2*, and *CrMTP3* cDNA sequences by RT-PCR from *C.*

reinhardtii CC125 RNA. First-strand cDNA was generated from 1 μg of DNase-treated RNA

using Superscript III reverse transcriptase (Life Technologies) and an oligo(dT) primer, then

KAPA HiFi DNA polymerase (Kapa Biosystems) and gene-specific primers were used for

each PCR amplification, with an annealing temperature of 60°C and 35 amplification cycles.

Following amplification, the PCR products were cloned into pGEM-T Easy plasmid

(Promega) for propagation and sequencing (GATC Biotech) to confirm sequence fidelity.

The yeast expression plasmid piUGpd (Nathan et al. 1999) was used to allow expression of

each cDNA under the control of the constitutive yeast GAPDH promoter and selection of the

URA3 gene. *CrMTP1* cDNA was sub-cloned into the XbaI and SacI sites of piUGpd, while

CrMTP2 and *CrMTP3* cDNA were sub-cloned into the BamHI and XbaI sites of piUGpd.

CrMTP4 in piUGpd was generated previously (Ibuot et al. 2017).

Quantitative gene expression analysis

C. reinhardtii CC125 was cultured in TAP medium for three days then cells were harvested

and frozen in liquid N$_2$. RNA was isolated and cDNA was produced as described above.

Expression for each MTP gene was determined by quantitative real-time PCR (qPCR) using

7

short amplicon primers that were designed to be specific to each gene (Supplementary Table S3). For qPCR a SYBR Green core qPCR kit (Eurogentec) and a StepOnePlus machine (ThermoFisher) using the SYBR Green detection program was used. Transcript abundance for each *MTP* was normalised to *CBLP* transcript abundance. Reactions were run in triplicate and qPCR analysis was performed as described previously (Bajhaiya et al. 2016).

Yeast heterologous expression and metal tolerance assays

Yeast (*S. cerevisiae*) strains *pmr1* (*MATa; his3Δ1; leu2Δ0; met15Δ0; ura3Δ0; pmr1*::*kanMX4*) (Euroscarf, Frankfurt, Germany), *zrc1 cot1* (*MATa; his3Δ1; leu2Δ0; met15Δ0; ura3Δ0; zrc1*::*natMX*; *cot1*::*kanMX4*) (Drager et al. 2004) (kindly provided by Ute Krämer) and the corresponding wild type strain BY4741 (*MATa; his3Δ1; leu2Δ0; met15Δ0; ura3Δ0*) (Euroscarf) were each transformed with each *MTP*-piUGpd plasmid or empty piUGpd plasmid using the lithium acetate-polyethylene glycol method. Colonies were selected by growth at 30°C in synthetic defined medium minus uracil (SD –Ura) as described previously (Pittman et al. 2004). Expression of each *MTP* cDNA in yeast was confirmed by RT-PCR using the appropriate *MTP* qPCR primer pair (Table S3) and RNA extracted from yeast using Trizol reagent, then RT-PCR was performed as described above. PCR products were examined on a 1% agarose gel stained with SafeView (NBS Biologicals).

Metal tolerance assays were performed essentially as described previously (Pittman et al. 2009) on solid SD –Ura medium with or without 2 mM $ZnCl_2$, 5 mM $MnCl_2$ or 0.8 mM $CoCl_2$ metal salts. For growth in liquid SD –Ura medium, yeast strains were grown in medium with or without 10 mM or 20 mM $CoCl_2$, $MnCl_2$, or $ZnCl_2$ metal salts. Cell density was determined by absorbance measurement at 600 nm while yeast biomass was determined by weighing a cell pellet from a set volume of culture after it was dried at 60°C for 24 h. Internal metal content in yeast grown in liquid SD –Ura medium containing 20 mM $ZnCl_2$ or 20 mM $MnCl_2$, respectively, was determined by inductively coupled plasma atomic emission spectroscopy (ICP-AES) essentially as described previously (Webster et al. 2011)

using a Perkin-Elmer Optima 5300. Cells were centrifuged for 10 min at 3000 g then resuspended in 10 mL of 1 mM EDTA for 5 min, then re-centrifuged and washed with 15 mL Milli-Q water. Cell pellets were dried at 60 °C for 24 h and then digested in 0.5 mL of ultrapure concentrated nitric acid at 70 °C for 2 h. Samples were diluted in Milli-Q water to 2% (v/v) concentration of acid and analysed by ICP-AES. Certified Reference Standard TM25.5 was used and all samples were calibrated using a matrix-matched serial dilution of Specpure multi-element plasma standard solution 4 (Alfa Aesar) set by linear regression.

Results

Phylogenetic analysis of algal CDF protein sequences

Previous phylogenetic analyses of CDF sequences are inconsistent in terms of clade structure and nomenclature of groups, with proposed numbers of CDF sub-groups ranging from 3 to 18 groups (Montanini et al. 2007; Migeon et al. 2010; Gustin et al. 2011; Cubillas et al. 2013). Montanini et al. (2007) divided the CDF family into three major groups based on substrate specificity, referred to as Zn-CDF, Fe/Zn-CDF and Mn-CDF, while Gustin et al. (2011) further sub-divided the higher plant CDF members into seven groups. Cubillas et al. (2013) identified 18 CDF groups that were differentiated mostly depending on whether they contained eukaryote, bacteria or archaea derived sequences. Here we performed a phylogenetic analysis that focussed on available algal genomes, including from one charophyte, 13 chlorophytes, two pelagophytes, two cryptophytes, three rhodophytes, four haptophytes, four bacillariophytes, three ochrophytes and one chlorarachniophyte (Table 1). A representative 'algal-like' thraustochytrid (*S. aggregatum*) was also included. First, each genome was analysed by a combination of BLAST and Pfam signature searching to collate CDF sequences. Each algal genome examined had at least one CDF sequence and the numbers of CDF transporter genes ranged from one in the red alga *G. sulphuraria* to 14 genes in the haptophyte bloom microalga *P. antarctica* (Table 1). The exact numbers of CDF genes within the more recently annotated genomes should be considered with caution since incorrect annotation and genome assembly errors can lead to genes being missed.

9

To generate the phylogenetic tree, the algal sequences were aligned with representative sequences from bacteria (*Escherichia coli*, *Bacillus subtilis*, *Bradyrhizobium diazoefficiens*, *Cupriavidus metallidurans*, *Rhizobium etli*, *Sinorhizobium meliloti*, *Streptococcus pneumoniae*, *Thermus thermophiles*), archaea (*Methanosarcina acetivorans*), cyanobacteria (*N. punctiforme*), animals (*H. sapiens*), fungi (*S. cerevisiae*), and land plants (*A. thaliana*), which had all been used in previous phylogenetic analyses and in most cases have known substrate specificity (Supplementary Table S1). The constructed phylogenetic tree contained 226 sequences, including 15 prokaryotic, 10 human, 12 plant, 6 yeast, 7 thraustochytrid and 176 algal sequences, of which 42 were chlorophyte sequences. Despite the dominance of many new algal sequences, the tree structure was consistent with previous CDF trees (Montanini et al. 2007; Gustin et al. 2011). It possessed distinct groups containing many of the known Zn^{2+}, Fe^{2+} and Mn^{2+} transporting CDF proteins characterised in human, yeast, *A. thaliana* and bacteria, which were recognisable as the previously named Zn-CDF, Fe/Zn-CDF and Mn-CDF groups (Figure 1). Group 1 (Zn-CDF) could have been considered as two or three separate groups, including a bacterial-specific clade (shown in dark blue in Figure 1) and two eukaryotic groups (an AtMTP1 – AtMTP4 containing group, and an AtMTP5 and AtMTP12 containing group), which all include CDF proteins with experimentally confirmed Zn^{2+} transport activity (e.g. MacDiarmid et al. 2002; Chao and Fu 2004; Kobae et al. 2004; Liuzzi and Cousins 2004; Arrivault et al. 2006; Fujiwara et al. 2015), indicating functional conservation across the whole Group 1. All taxonomic classes of algae possessed a Group 1 Zn-CDF, apart from the Chlorarachniophyta *B. natans*, although 5 of the 13 chlorophytes, including all three *Ostreococcus* spp. appear to lack a Zn-CDF (Table 1).

Group 2 (Fe/Zn-CDF), which includes Fe^{2+} and/or Zn^{2+} transporting proteins such as yeast ScMMT1 and ScMMT2, and *C. metallidurans* CmFieF, is rich in algal CDF sequences, including a large number of haptophyte, bacillariophyte, and ochrophyte sequences, but includes only two chlorophyte and no rhodophyte sequences (Figure 1). A predominantly bacterial sub-group also containing five algal sequences (shown in light green in Figure 1)

10

might be considered as a separate group since it contains CDF proteins with known Mn^{2+}, Ni^{2+} and Co^{2+} transport activities (Cubillas et al. 2013) rather than Fe^{2+}/Zn^{2+}. Group 3 and Group 4 (Mn-CDF) are considered as two separate groups rather than a single group. Group 4 contains many known plant Mn^{2+} transporting CDFs, such as AtMTP11 (Delhaize et al. 2007; Peiter et al. 2007) and is also enriched in chlorophyte and haptophyte sequences. Group 3 is also rich in sequences from all chlorophyte species, and includes CDF proteins such as AtMTP7 and HsZnt9 that have no currently confirmed substrate (Figure 1). Although indirect evidence indicates Zn^{2+} transport activity by HsZnt9 (Perez et al. 2017), Group 3 is referred to as a separate undefined CDF group. Finally, the tree displays a fifth algal-specific group, which is also referred to as undefined. Group 5 sequences are missing in all of the examined higher plant, charophyte and chlorophyte genomes (Supplementary Figure S1).

In order to provide validation for the group structure proposed for the CDF tree shown in Figure 1, a phenetic sequence clustering method was performed using CLANS (Frickey and Lupas 2004). Nearly all of the sequences fell into five clusters, which completely matched the Groups 1 to 5 determined by the phylogenetic tree (Figure 2). In particular, the analysis fully validated the separation of Group 3 and 4 into independent groups, which were both very tightly clustered. The Group 2 sequences were fairly tightly clustered and indicated partly that this group should not be further divided (shown by light green and dark green symbols overlapping in Figure 2), although six of the sequences within this sub-group, including five algal proteins from *Pelagophyceae* sp., *T. pseudonana*, *E. siliculosus* and *Ochromonadaceae* sp., and the bacterial Sm_0683 protein from *S. meliloti* did not cluster with the other Group 2 sequences, and are instead classified as 'unassigned' (Table 1). Group 1 and 5 sequences also formed clearly distinct clusters although these were not as tightly clustered as the other groups, and there was some overlap between four of the Group 5 sequences with Group 1. Overall, this CLANS analysis validated the five-group organisation for these CDF sequences.

11

Structural features of Zn-CDF related sequences from algae

Conserved amino acid residues within TMD2 and 5 have been demonstrated to be critical for metal ion binding, in particular, two residues from TMD2 and two from TMD5 form a metal binding site referred to as 'binding site A' (Kolaj-Robin et al. 2015; Barber-Zucker et al. 2017). The presence of residues HxxxD-HxxxD within the TMD2 and TMD5 regions, respectively, was conserved for the algal-dominated Group 1 proteins examined here (Figure 3), which is consistent with previous analysis of Zn-CDF proteins (Montanini et al. 2007). In contrast, the Group 5 proteins displayed a binding site A motif that was predominantly A/SxxxD-HxxxD, such that Ala or Ser replaced the conserved His (Figure 3). Only 4 of the 26 Group 5 proteins had the HxxxD-HxxxD motif that was highly conserved within Group 1 proteins. Indeed, these were the four Group 5 proteins that partially overlapped with the Group 1 cluster (Figure 2).

Most of the Zn^{2+}-transporting CDF proteins within Group 1 possess a His-rich cytosolic loop between TMD4 and 5, and this loop may play a role in metal selectivity, as some Zn-CDF transporters are specific for Zn^{2+} while others can also transport metals including Co^{2+} (Kawachi et al. 2012; Podar et al. 2012). However, the presence of a His-rich sequence is not universal, and while most the Zn-CDF proteins examined here possess an obvious His-rich loop region, including most of the chlorophyte and bacillariophyte sequences, a few do not, including some of the human Znt proteins, *A. thaliana* AtMTP5, and AtMTP5-related algal sequences (Figure 4a). Another notable feature of many of the algal Zn-CDF sequences is that the His-rich cytosolic loop is often significantly longer than the equivalent loop region present within CDF proteins such as from *Arabidopsis*, human and yeast (Figure 4b). For example, the CrMTP1 His-rich loop is over 300 amino acids in length while the AtMTP1 loop just over 50 amino acids in length (Supplementary Figure S2). However, some algal CDF proteins, such as from *Micromonas* sp. and *G. theta* have very short His-stretch regions of less than 10 amino acids (Figure 4b).

Functional characterisation of *C. reinhardtii* CDF proteins

C. reinhardtii has five CDF proteins, CrMTP1 within Group 1 (Zn-CDF), CrMTP2, CrMTP3 and CrMTP4, within Group 4 (Mn-CDF), and CrMTP5 within the undefined Group 3 (Supplementary Figure S1). To determine whether all genes are expressed within the organism, RT-PCR was performed using RNA extracted from exponential growth stage cells grown under standard conditions. Transcripts were detected for all five genes with *CrMTP1*, *CrMTP2* and *CrMTP5* showing an equivalent level of expression while *CrMTP3* and *CrMTP4* had low but detectable expression (Figure 5). Growth of *C. reinhardtii* in excess concentrations of metals such as Cd, Co, Fe, Mn and Zn had no significant effect on the expression level of any of the genes (data not shown) indicating that none of these CrMTP genes are transcriptionally regulated by excess metal status.

CrMTP4 has previously been confirmed to have Mn^{2+} transport activity and the ability to transport Cd^{2+} (Ibuot et al. 2017) but the substrate specificity of the other *C. reinhardtii* CDF proteins is unknown. The full-length cDNA for each gene was functionally characterised by heterologous expression in yeast (Figure 6), however, the expression of CrMTP5 was unsuccessful and therefore no functional information could be obtained for this protein. In contrast, CrMTP1, CrMTP2, CrMTP3 and CrMTP4 were all successfully expressed in a Zn- and Co-sensitive yeast strain *zrc1 cot1* (lacking the yeast vacuolar Zn^{2+} and Co^{2+} transporters ScZRC1 and ScCOT1, respectively), and a Mn-sensitive yeast strain *pmr1* (lacking the Mn^{2+} ATPase transporter ScPMR1) (Figure 6b). All cDNAs were functional as indicated by their ability to suppress metal sensitive phenotypes (Figure 6a). CrMTP4 was used as a positive control as a confirmed Mn-CDF, and as seen with other higher plant Mn-CDF proteins, it was unable to rescue the growth of *zrc1 cot1* yeast on Zn or Co media. In contrast, CrMTP1 could strongly suppress both the Zn and Co sensitivity of *zrc1 cot1* but was unable to suppress the Mn sensitivity of *pmr1*, indicating that CrMTP1 is a Zn^{2+} and Co^{2+} transporter. CrMTP2 showed the identical characteristics of CrMTP4, indicating that it is a specific Mn^{2+} transporter (Figure 6a). CrMTP3 was interesting as it could strongly suppress the Mn sensitivity of *pmr1* but could also partially suppress the Zn and Co sensitivity of *zrc1*

13

cot1, although not as strongly as CrMTP1. This suggested that CrMTP3 has broad substrate specificity for all three divalent cations tested. To date, none of the Mn-CDF proteins have been found to have Zn^{2+} or Co^{2+} transport activity, and appear to be largely Mn^{2+}-specific (Delhaize et al. 2007; Montanini et al. 2007; Peiter et al. 2007).

To further confirm the Zn, Co and Mn tolerance abilities of these proteins all cDNAs were expressed in a wild type yeast strain (BY4741) (Figure 6b) and growth of the yeast in liquid medium was quantified in the presence of external metal addition. CrMTP1 but not CrMTP3 was able to moderately but significantly increase tolerance to Zn in the yeast strain as determined by cell density measurement (Figure 7b) and by yeast biomass (Figure 8a). However, there was no significant increase in yeast growth for any of the MTP-expressing strains in response to Co addition (Figure 7c and Figure 8b). All three CDF proteins (CrMTP2, CrMTP3, CrMTP4) that were able to strongly suppress the Mn sensitivity of *pmr1* yeast could also provide strong growth tolerance to BY4741 yeast in the presence of 20 mM Mn (Figure 7d and Figure 8c).

Metal accumulation into yeast expressing *C. reinhardtii* CDF proteins

To determine whether the expression of algal CDF proteins in yeast can provide increased metal transport into the cell, Zn and Mn concentration in yeast cell biomass was quantified by ICP-AES following growth in liquid media with added Zn or Mn. Prior to measurement, cells were washed in an EDTA solution to remove cell wall bound metals so that only internalised metals were measured. There was no significant increase in Zn content for any of the strains including for the CrMTP1 expressing yeast (Figure 9a), whereas the yeast expressing CrMTP2, CrMTP3 and CrMTP4 showed an approximately 2-fold increase in Mn content within the cells (Figure 9b), indicating that the Mn tolerance of these strains was potentially due to internal sequestration of Mn.

14

Discussion

CDF metal transporters are a ubiquitous family of proteins across life, and this analysis confirms their presence across the wide range of taxonomically and physiologically diverse photosynthetic organisms that are collectively referred to as algae. CDF transporters appear to be principally involved in the transfer of various essential metal ions including Zn^{2+}, Mn^{2+}, Fe^{2+} and Co^{2+} into internal organelles either for delivery to specific subcellular-localised proteins that require metal co-factors or for providing metal tolerance through internal sequestration (Ricachenevsky et al. 2013; Kolaj-Robin et al. 2015). Although other classes of primary or secondary energised metal transporters can play similar roles (Blaby-Haas and Merchant 2012), CDF transporters are clearly indispensable in algae since each algal genome that has been analysed here has at least one CDF isoform. Furthermore, the algal-dominated phylogenetic analysis performed in this study was consistent with a previously determined CDF phylogenetic structure, whereby a small number of major groups can be differentiated on the basis of Zn^{2+}, Fe^{2+}/Zn^{2+} and Mn^{2+} substrate specificity, plus undefined substrate specificity (Montanini et al. 2007). The fact that this phylogenetic structure is conserved in many algal species suggests that it was determined early in the evolution of photosynthetic organisms. In particular, the Zn-CDF and Mn-CDF groups are the most conserved across the algal genomes examined here. Nevertheless, some algal species have lost particular CDF types; for example, all three *Ostreococcus* spp. lack Group 1 (Zn-CDF) and Group 2 (Fe/Zn-CDF) genes, and in fact most chlorophytes lack Group 2 (Fe/Zn-CDF) genes, while all three red algae examined (*C. merolae*, *G. sulphuraria* and *P. umbilicalis*) lack Group 2 (Fe/Zn-CDF) and the undefined Group 3 genes. The functional relevance of this is unclear but may indicate that functional redundancy with other transporter classes (e.g. Zn^{2+} or Mn^{2+} P-type ATPases; Fe^{2+} or Mn^{2+} transporting VIT-like proteins) is not essential and such redundancy has therefore not been selected in many of these organisms.

We have also proposed the presence of a fifth phylogenetic group (Group 5) that is most closely related to Group 1 (Zn-CDF) but appears to be distinct. This group is almost

15

exclusively algal-specific apart from a *S. aggregatum* isoform, but includes no chlorophyte or rhodophyte sequences. The difference in sequence for the TMD2 half of the metal binding site A motif of the majority of the Group 5 proteins further demonstrates a divergence with the other groups. This TMD2 motif is typically HxxxD or DxxxD in most CDF proteins, such as in the Zn^{2+}-transporting AtMTP1 and CrMTP1 (HxxxD), and in the Mn^{2+}-transporting AtMTP11 and CrMTP4 (DxxxD), but the Group 5 TMD2 motif was A/SxxxD. Mutation of the His residue within this motif to Ala in the AtMTP1 Zn-CDF protein, the PtdMTP1 Zn-CDF protein from *Populus trichocarpa x deltoides* and the RmCzcD Zn-CDF protein from *Ralstonia metallidurans* all caused loss of function (Blaudez et al. 2003; Anton et al. 2004; Kawachi et al. 2012), perhaps indicating that these Group 5 proteins would not be functional for Zn^{2+} transport. However, there are exceptions to these motifs where His or Asp in the first position is not essential, such as NxxxD within TMD2 of the Mn^{2+} transporting SpMntA from *S. pneumoniae* or FxxxD within TMD2 of the Zn^{2+} transporting ScZRG17 from *S. cerevisiae* (Barber-Zucker et al. 2017). Furthermore, the recently identified Na^+-transporting MceT protein from the halophilic bacterium *Planococcus dechangensis*, which has been proposed to be a member of a novel Na-CDF clade, has a distinct YxxxS motif (Xu et al. 2019). Currently we are unable to predict the substrate specificity of these Group 5 algae proteins from sequence comparisons therefore future experimental analysis is needed.

This study has identified *C. reinhardtii* members of the CDF family of metal efflux transporters as Zn^{2+}, Co^{2+} and Mn^{2+} transporters, and validated the function of an algal Zn-CDF protein for the first time. CrMTP1 clearly groups in the Group 1 (Zn-CDF) clade while CrMTP2, CrMTP3 and CrMTP4 are clearly within the Group 4 (Mn-CDF) clade, and the yeast expression experiments validated these predicted activities, as we previously observed for CrMTP4 (Ibuot et al. 2017). An intriguing exception was the apparent Mn^{2+} and Zn^{2+} transport activity by CrMTP3, the first example we are aware of for a Mn^{2+}-transporting CDF also being linked to Zn^{2+} transport. A Mn-CDF from *A. thaliana* (AtMTP8) may transport both Mn^{2+} and Fe^{2+} (Chu et al. 2017), while the Group 1 (Zn-CDF) member HsZnt10 can transport Mn^{2+} (Nishito et al. 2016). While there is some sequence variation between

16

CrMTP3 and CrMTP2/CrMTP4 that could explain this difference, future biochemical and mutagenesis studies are required to experimental validate this further.

CrMTP1 was able to efficiently provide Zn tolerance to yeast, indicating Zn^{2+} transport activity, despite the structure of CrMTP1 being distinct from previously characterised Zn-CDF proteins such as AtMTP1 and ScZRC1 due to the significantly longer His-rich loop domain between TMD4 and 5. This seems to be a structural feature for many of the algal Zn-CDF proteins. The His-rich loop has been proposed to play a role in metal ion specificity and affinity, such that shortening of the AtMTP1 loop, which also reduces the number of His residues, alters the kinetics of Zn^{2+} transport, while the shortened loop or specific point-mutations within the loop can allow Co^{2+} transport, which is otherwise poor in native AtMTP1 (Kawachi et al. 2008; Podar et al. 2012). Therefore we might predict that the longer His-loop of CrMTP1 may provide different Zn^{2+} and Co^{2+} transport kinetics compared to some of the higher plant isoforms.

CrMTP2 and *CrMTP4* but not the other *C. reinhardtii* CDF family genes have been shown to be transcriptionally induced by Mn deficiency, thus linking them further to Mn homeostasis roles (Allen et al. 2007), while *CrMTP1* is induced by Zn deficiency (Malasarn et al. 2013), although we could find no evidence by RT-PCR that any of these genes are transcriptionally regulated by metal excess. CrMTP1 was able to efficiently rescue the Zn sensitive phenotype of the yeast vacuolar Zn^{2+}/H^+ CDF transporter ScZRC1 and provide Zn tolerance in wild type yeast, thus it is proposed to provide a pathway of vacuolar Zn^{2+} sequestration equivalent to AtMTP1 and ScZRC1 (MacDiarmid et al. 2002; Kobae et al. 2004). Likewise, the significant Mn tolerance gained by CrMTP2, CrMTP3 or CrMTP4 that was coincident with increased Mn content within the cell is consistent with sequestration of Mn^{2+} into an internal compartment, possibly a vacuolar structure. *C. reinhardtii* lacks a large central vacuole as in typical plant cells but possess multiple lysosomal/vacuolar-like structures that are also referred to as acidocalcisomes (Komine et al. 2000; Blaby-Haas and Merchant 2014). These are acidic structures that accumulate polyphosphate and metals including Ca, Mg and Zn, and possess proton pumps that would be able to energise H^+-

17

coupled Zn^{2+} or Mn^{2+} transport by an MTP protein (Ruiz et al. 2001). The identification of the red algal MTP1 orthologue from *C. merolae* (Cmer_CMF058C) from an acidocalcisome proteomic study (Yagisawa et al. 2009) further strengthens the likely function of algal Zn-CDF proteins in vacuolar Zn^{2+} sequestration.

Knowledge of sub-cellular metal transport processes, such as by members of the CDF transporter family, not only provides improved understanding of fundamental mechanisms of metal homeostasis and metal tolerance within a cell for a given organism, but may provide tools for biotechnological approaches to manipulate metal content within a whole organism, tissue, or sub-cellular compartment. Previous studies have proposed applications of CDF transporters for enhancing mineral biofortification of plants or for providing toxic metal bioremediation in plants or algae (Ricachenevsky et al. 2013; Das et al. 2016; Ibuot et al. 2017). This present study has indicated the wide diversity of CDF transporters that exist within the algae lineage. Although the vast majority of these proteins are still uncharacterized and the potential metal substrates are unknown, it is quite possible that some of these proteins will have characteristics that are distinct to those CDF transporters already known in plants and other eukaryotes. Therefore algal CDF genes may be attractive gene targets for future genetic engineering approaches in plants or microorganisms for metal transport engineering.

Acknowledgements

References

Allen MD, Kropat J, Tottey S, Del Campo JA, Merchant SS (2007) Manganese deficiency in Chlamydomonas results in loss of photosystem II and MnSOD function, sensitivity to

peroxides, and secondary phosphorus and iron deficiency. Plant Physiol 143 (1):263-277. doi:10.1104/pp.106.088609

Andreini C, Bertini I, Cavallaro G, Holliday GL, Thornton JM (2008) Metal ions in biological catalysis: from enzyme databases to general principles. J Biol Inorg Chem 13 (8):1205-1218. doi:10.1007/s00775-008-0404-5

Anton A, Weltrowski A, Haney CJ, Franke S, Grass G, Rensing C, Nies DH (2004) Characteristics of zinc transport by two bacterial Cation Diffusion Facilitators from *Ralstonia metallidurans* CH34 and *Escherichia coli*. J Bacteriol 186 (22):7499-7507. doi:10.1128/jb.186.22.7499-7507.2004

Antosiewicz DM, Barabasz A, Siemianowski O (2014) Phenotypic and molecular consequences of overexpression of metal-homeostasis genes. Front Plant Sci 5:80. doi:10.3389/fpls.2014.00080

Arrivault S, Senger T, Kramer U (2006) The Arabidopsis metal tolerance protein AtMTP3 maintains metal homeostasis by mediating Zn exclusion from the shoot under Fe deficiency and Zn oversupply. Plant J 46 (5):861-879. doi:10.1111/j.1365-313X.2006.02746.x

Bajhaiya AK, Dean AP, Zeef LAH, Webster RE, Pittman JK (2016) PSR1 Is a Global Transcriptional Regulator of Phosphorus Deficiency Responses and Carbon Storage Metabolism in Chlamydomonas reinhardtii. Plant Physiology 170 (3):1216-1234. doi:10.1104/pp.15.01907

Barber-Zucker S, Shaanan B, Zarivach R (2017) Transition metal binding selectivity in proteins and its correlation with the phylogenomic classification of the cation diffusion facilitator protein family. Sci Rep 7 (1):16381. doi:10.1038/s41598-017-16777-5

Blaby-Haas CE, Merchant SS (2012) The ins and outs of algal metal transport. Biochimica et Biophysica Acta 1823 (9):1531-1552. doi:10.1016/j.bbamcr.2012.04.010

Blaby-Haas CE, Merchant SS (2014) Lysosome-related organelles as mediators of metal homeostasis. J Biol Chem 289 (41):28129-28136. doi:10.1074/jbc.R114.592618

19

Blaby-Haas CE, Merchant SS (2017) Regulating cellular trace metal economy in algae. Curr Opin Plant Biol 39:88-96. doi:https://doi.org/10.1016/j.pbi.2017.06.005

Blaudez D, Kohler A, Martin F, Sanders D, Chalot M (2003) Poplar metal tolerance protein 1 confers zinc tolerance and is an oligomeric vacuolar zinc transporter with an essential leucine zipper motif. Plant Cell 15 (12):2911-2928

Chao Y, Fu D (2004) Kinetic study of the antiport mechanism of an *Escherichia coli* zinc transporter, ZitB. J Biol Chem 279 (13):12043-12050. doi:10.1074/jbc.M313510200

Cheng SY, Show P-L, Lau BF, Chang J-S, Ling TC (2019) New prospects for modified algae in heavy metal adsorption. Trends Biotechnol 37 (11):1255-1268. doi:https://doi.org/10.1016/j.tibtech.2019.04.007

Chu H-H, Car S, Socha AL, Hindt MN, Punshon T, Guerinot ML (2017) The Arabidopsis MTP8 transporter determines the localization of manganese and iron in seeds. Scientific Reports 7 (1):11024. doi:10.1038/s41598-017-11250-9

Crooks GE, Hon G, Chandonia J-M, Brenner SE (2004) WebLogo: a sequence logo generator. Genome Res 14 (6):1188-1190. doi:10.1101/gr.849004

Cubillas C, Vinuesa P, Tabche ML, García-de los Santos A (2013) Phylogenomic analysis of Cation Diffusion Facilitator proteins uncovers Ni^{2+}/Co^{2+} transporters. Metallomics 5 (12):1634-1643. doi:10.1039/C3MT00204G

Das N, Bhattacharya S, Maiti MK (2016) Enhanced cadmium accumulation and tolerance in transgenic tobacco overexpressing rice metal tolerance protein gene OsMTP1 is promising for phytoremediation. Plant Physiol Biochem 105:297-309. doi:https://doi.org/10.1016/j.plaphy.2016.04.049

Delhaize E, Gruber BD, Pittman JK, White RG, Leung H, Miao YS, Jiang LW, Ryan PR, Richardson AE (2007) A role for the AtMTP11 gene of *Arabidopsis* in manganese transport and tolerance. Plant J 51 (2):198-210

Drager DB, Desbrosses-Fonrouge AG, Krach C, Chardonnens AN, Meyer RC, Saumitou-Laprade P, Kramer U (2004) Two genes encoding *Arabidopsis halleri* MTP1 metal

20

transport proteins co-segregate with zinc tolerance and account for high *MTP1* transcript levels. Plant J 39 (3):425-439. doi:10.1111/j.1365-313X.2004.02143.x

Ellis CD, MacDiarmid CW, Eide DJ (2005) Heteromeric protein complexes mediate zinc transport into the secretory pathway of eukaryotic cells. J Biol Chem 280 (31):28811-28818. doi:10.1074/jbc.M505500200

Emery L, Whelan S, Hirschi KD, Pittman JK (2012) Protein phylogenetic analysis of Ca^{2+}/cation antiporters and insights into their evolution in plants. Front Plant Sci 3:1. doi:10.3389/fpls.2012.00001

Eroglu S, Meier B, von Wirén N, Peiter E (2016) The vacuolar manganese transporter MTP8 determines tolerance to iron deficiency-induced chlorosis in Arabidopsis. Plant Physiol 170 (2):1030-1045. doi:10.1104/pp.15.01194

Frickey T, Lupas A (2004) CLANS: a Java application for visualizing protein families based on pairwise similarity. Bioinformatics 20 (18):3702-3704. doi:10.1093/bioinformatics/bth444

Fujiwara T, Kawachi M, Sato Y, Mori H, Kutsuna N, Hasezawa S, Maeshima M (2015) A high molecular mass zinc transporter MTP12 forms a functional heteromeric complex with MTP5 in the Golgi in *Arabidopsis thaliana*. FEBS J 282 (10):1965-1979. doi:10.1111/febs.13252

Gustin JL, Zanis MJ, Salt DE (2011) Structure and evolution of the plant cation diffusion facilitator family of ion transporters. BMC Evol Biol 11 (1):76. doi:10.1186/1471-2148-11-76

Haney CJ, Grass G, Franke S, Rensing C (2005) New developments in the understanding of the cation diffusion facilitator family. J Ind Microbiol Biotechnol 32 (6):215-226. doi:10.1007/s10295-005-0224-3

Hanikenne M, Kramer U, Demoulin V, Baurain D (2005) A comparative inventory of metal transporters in the green alga *Chlamydomonas reinhardtii* and the red alga *Cyanidioschizon merolae*. Plant Physiol 137 (2):428-446. doi:10.1104/pp.104.054189

Harris EH (1989) The Chlamydomonas Sourcebook. Academic Press, San Diego

Ibuot A, Dean AP, McIntosh OA, Pittman JK (2017) Metal bioremediation by CrMTP4 over-expressing *Chlamydomonas reinhardtii* in comparison to natural wastewater-tolerant microalgae strains. Algal Res 24:89-96. doi:https://doi.org/10.1016/j.algal.2017.03.002

Kawachi M, Kobae Y, Kogawa S, Mimura T, Kraemer U, Maeshima M (2012) Amino acid screening based on structural modeling identifies critical residues for the function, ion selectivity and structure of Arabidopsis MTP1. FEBS J 279 (13):2339-2356. doi:10.1111/j.1742-4658.2012.08613.x

Kawachi M, Kobae Y, Mimura T, Maeshima M (2008) Deletion of a histidine-rich loop of AtMTP1, a vacuolar Zn^{2+}/H^+ antiporter of *Arabidopsis thaliana*, stimulates the transport activity. J Biol Chem 283 (13):8374-8383. doi:10.1074/jbc.M707646200

Kobae Y, Uemura T, Sato MH, Ohnishi M, Mimura T, Nakagawa T, Maeshima M (2004) Zinc transporter of *Arabidopsis thaliana* AtMTP1 is localized to vacuolar membranes and implicated in zinc homeostasis. Plant Cell Physiol 45 (12):1749-1758. doi:10.1093/pcp/pci015

Kolaj-Robin O, Russell D, Hayes KA, Pembroke JT, Soulimane T (2015) Cation Diffusion Facilitator family: Structure and function. FEBS Lett 589 (12):1283-1295. doi:https://doi.org/10.1016/j.febslet.2015.04.007

Komine Y, Eggink LL, Park HS, Hoober JK (2000) Vacuolar granules in *Chlamydomonas reinhardtii*: polyphosphate and a 70-kDa polypeptide as major components. Planta 210 (6):897-905

Kramer U, Talke IN, Hanikenne M (2007) Transition metal transport. FEBS Lett 581 (12):2263-2272. doi:10.1016/j.febslet.2007.04.010

Krogh A, Larsson B, von Heijne G, Sonnhammer ELL (2001) Predicting transmembrane protein topology with a hidden Markov model: Application to complete genomes. J Mol Biol 305 (3):567-580. doi:10.1006/jmbi.2000.4315

Li L, Miao R, Jia X, Ward DM, Kaplan J (2014) Expression of the yeast Cation Diffusion Facilitators Mmt1 and Mmt2 affects mitochondrial and cellular iron homeostasis: evidence

22

for mitochondrial iron export. J Biol Chem 289 (24):17132-17141.

doi:10.1074/jbc.M114.574723

Liuzzi JP, Cousins RJ (2004) Mammalian zinc transporters. Annu Rev Nutr 24 (1):151-172.

doi:10.1146/annurev.nutr.24.012003.132402

MacDiarmid CW, Milanick MA, Eide DJ (2002) Biochemical properties of vacuolar zinc

transport systems of *Saccharomyces cerevisiae*. J Biol Chem 277 (42):39187-39194

Madeira F, Park Ym, Lee J, Buso N, Gur T, Madhusoodanan N, Basutkar P, Tivey ARN,

Potter SC, Finn RD, Lopez R (2019) The EMBL-EBI search and sequence analysis tools

APIs in 2019. Nucleic Acids Res 47 (W1):W636-W641. doi:10.1093/nar/gkz268

Malasarn D, Kropat J, Hsieh SI, Finazzi G, Casero D, Loo JA, Pellegrini M, Wollman F-A,

Merchant SS (2013) Zinc deficiency impacts CO_2 assimilation and disrupts copper

homeostasis in *Chlamydomonas reinhardtii*. J Biol Chem 288 (15):10672-10683.

doi:10.1074/jbc.M113.455105

Migeon A, Blaudez D, Wilkins O, Montanini B, Campbell MM, Richaud P, Thomine S, Chalot

M (2010) Genome-wide analysis of plant metal transporters, with an emphasis on poplar.

Cell Mol Life Sci 67 (22):3763-3784. doi:10.1007/s00018-010-0445-0

Montanini B, Blaudez D, Jeandroz S, Sanders D, Chalot M (2007) Phylogenetic and

functional analysis of the Cation Diffusion Facilitator (CDF) family: improved signature

and prediction of substrate specificity. BMC Genomics 8 (1):107. doi:10.1186/1471-2164-

8-107

Nathan DF, Vos MH, Lindquist S (1999) Identification of SSF1, CNS1, and HCH1 as

multicopy suppressors of a Saccharomyces cerevisiae Hsp90 loss-of-function mutation.

Proc Natl Acad Sci USA 96 (4):1409-1414

Nies DH, Silver S (1995) Ion efflux systems involved in bacterial metal resistances. J Ind

Microbiol 14 (2):186-199. doi:10.1007/bf01569902

Nishito Y, Tsuji N, Fujishiro H, Takeda T-a, Yamazaki T, Teranishi F, Okazaki F, Matsunaga

A, Tuschl K, Rao R, Kono S, Miyajima H, Narita H, Himeno S, Kambe T (2016) Direct

comparison of manganese detoxification/efflux proteins and molecular characterization of

23

ZnT10 protein as a manganese transporter. J Biol Chem 291 (28):14773-14787. doi:10.1074/jbc.M116.728014

Peiter E, Montanini B, Gobert A, Pedas P, Husted S, Maathuis FJM, Blaudez D, Chalot M, Sanders D (2007) A secretory pathway-localized cation diffusion facilitator confers plant manganese tolerance. Proc Natl Acad Sci USA 104 (20):8532-8537

Perez Y, Shorer Z, Liani-Leibson K, Chabosseau P, Kadir R, Volodarsky M, Halperin D, Barber-Zucker S, Shalev H, Schreiber R, Gradstein L, Gurevich E, Zarivach R, Rutter GA, Landau D, Birk OS (2017) SLC30A9 mutation affecting intracellular zinc homeostasis causes a novel cerebro-renal syndrome. Brain 140 (4):928-939. doi:10.1093/brain/awx013

Pittman JK, Cheng NH, Shigaki T, Kunta M, Hirschi KD (2004) Functional dependence on calcineurin by variants of the *Saccharomyces cerevisiae* vacuolar Ca^{2+}/H^+ exchanger Vcx1p. Mol Microbiol 54 (4):1104-1116

Pittman JK, Edmond C, Sunderland PA, Bray CM (2009) A cation-regulated and proton gradient-dependent cation transporter from *Chlamydomonas reinhardtii* has a role in calcium and sodium homeostasis. J Biol Chem 284 (1):525-533. doi:10.1074/jbc.M807173200

Pittman JK, Hirschi KD (2016) Phylogenetic analysis and protein structure modelling identifies distinct Ca^{2+}/Cation antiporters and conservation of gene family structure within Arabidopsis and rice species. Rice 9 (1):3. doi:10.1186/s12284-016-0075-8

Podar D, Scherer J, Noordally Z, Herzyk P, Nies D, Sanders D (2012) Metal selectivity determinants in a family of transition metal transporters. J Biol Chem 287 (5):3185-3196. doi:10.1074/jbc.M111.305649

Ricachenevsky F, Menguer P, Sperotto R, Williams L, Fett J (2013) Roles of plant metal tolerance proteins (MTP) in metal storage and potential use in biofortification strategies. Front Plant Sci 4:144. doi:10.3389/fpls.2013.00144

Ruiz FA, Marchesini N, Seufferheld M, Govindjee, Docampo R (2001) The polyphosphate

bodies of *Chlamydomonas reinhardtii* possess a proton-pumping pyrophosphatase and

are similar to acidocalcisomes. J Biol Chem 276 (49):46196-46203

Sharma SS, Dietz K-J, Mimura T (2016) Vacuolar compartmentalization as indispensable

component of heavy metal detoxification in plants. Plant, Cell Environ 39 (5):1112-1126.

doi:10.1111/pce.12706

Stamatakis A (2006) RAxML-VI-HPC: Maximum likelihood-based phylogenetic analyses with

thousands of taxa and mixed models. Bioinformatics 22 (21):2688-2690.

doi:10.1093/bioinformatics/btl446

Stamatakis A, Hoover P, Rougemont J (2008) A rapid bootstrap algorithm for the RAxML

web servers. Syst Biol 57 (5):758-771. doi:10.1080/10635150802429642

Suresh Kumar K, Dahms H-U, Won E-J, Lee J-S, Shin K-H (2015) Microalgae – A promising

tool for heavy metal remediation. Ecotoxicol Environ Saf 113:329-352.

doi:https://doi.org/10.1016/j.ecoenv.2014.12.019

Tsirigos KD, Peters C, Shu N, Käll L, Elofsson A (2015) The TOPCONS web server for

consensus prediction of membrane protein topology and signal peptides. Nucleic Acids

Res 43 (W1):W401-W407. doi:10.1093/nar/gkv485

Webster RE, Dean AP, Pittman JK (2011) Cadmium exposure and phosphorus limitation

increases metal content in the freshwater alga *Chlamydomonas reinhardtii*. Environ Sci

Technol 45 (17):7489-7496. doi:10.1021/es200814c

Xu T, Chen H, Li J, Hong S, Shao L, Zheng X, Zou Q, Wang Y, Guo S, Jiang J (2019)

Implications for cation selectivity and evolution by a novel Cation Diffusion Facilitator

family member from the moderate halophile *Planococcus dechangensis*. Front Microbiol

10:607. doi:10.3389/fmicb.2019.00607

Yagisawa F, Nishida K, Yoshida M, Ohnuma M, Shimada T, Fujiwara T, Yoshida Y, Misumi

O, Kuroiwa H, Kuroiwa T (2009) Identification of novel proteins in isolated polyphosphate

vacuoles in the primitive red alga *Cyanidioschyzon merolae*. Plant J 60 (5):882-893.

doi:10.1111/j.1365-313X.2009.04008.x

Zimmermann L, Stephens A, Nam S-Z, Rau D, Kübler J, Lozajic M, Gabler F, Söding J,

Lupas AN, Alva V (2018) A completely reimplemented MPI Bioinformatics Toolkit with a

new HHpred server at its core. J Mol Biol 430 (15):2237-2243.

doi:https://doi.org/10.1016/j.jmb.2017.12.007

Table 1. Total number and distribution of CDF transporter genes from each analysed genome into five phylogenetic groups: Group 1 (Zn-CDF), Group 2 (Fe/Zn-CDF), Group 3 (undefined CDF), Group 4 (Mn-CDF), Group 5 (undefined CDF). Gene numbers were determined from the phylogenetic analysis (Figure 1) and supported by the cluster analysis (Figure 2). Six sequences were classed as unassigned (UA) including five sequences where the evidence for Group 2 assignment was not supported by cluster analysis.

|	Species	G.1 (Zn)	G.2 (Fe/Zn)	G.3 (n.d.)	G.4 (Mn)	G.5 (n.d.)	UA	Total
Cyanobacteria	*Nostoc punctiforme*	0	2	2	0	0	0	4
Metazoa	*Homo sapiens*	9	0	1	0	0	0	10
Ascomycota	*Saccharomyces cerevisiae*	3	2	0	0	0	1	6
Embryophyta	*Arabidopsis thaliana*	6	1	1	4	0	0	12
Thraustochytrid	*Schizochytrium aggregatum*	3	1	1	1	1	0	7
Charophyta	*Klebsormidium nitens*	4	1	1	2	0	0	8
Chlorophyta	*Bathycoccus prasinos*	0	1	1	1	0	0	3
	Botryococcus braunii	1	0	1	0	0	0	2
	Chlamydomonas reinhardtii	1	0	1	3	0	0	5
	Chlorella sp. NC64A	1	0	1	1	0	0	3
	Chromochloris zofingiensis	1	0	1	2	0	0	4
	Coccomyxa subellipsoidea	2	0	1	2	0	0	5
	Dunaliella salina	2	0	1	1	0	0	4
	Micromonas pusilla	0	0	1	1	0	0	2
	Micromonas sp.	2	1	1	1	0	0	5
	Ostreococcus lucimarinus	0	0	1	1	0	0	2
	Ostreococcus sp.	0	0	1	1	0	0	2
	Ostreococcus tauri	0	0	1	1	0	0	2
	Volvox carteri	1	0	1	1	0	0	3
Pelagophyta	*Aureococcus anophagefferens*	1	2	0	1	0	0	4
	Pelagophyceae sp.	1	2	1	2	4	1	11
Cryptophyta	*Cryptophyceae* sp.	1	1	0	0	1	0	3
	Guillardia theta	6	1	1	1	1	0	10
Rhodophyta	*Cyanidioschyzon merolae*	2	0	0	1	0	0	3
	Galdieria sulphuraria	1	0	0	0	0	0	1
	Porphyra umbilicalis	3	0	0	1	0	0	4
Haptophyta	*Emiliania huxleyi*	3	4	0	1	3	0	11
	Pavlovales sp.	2	2	0	2	3	0	9
	Phaeocystis antarctica	5	7	1	1	0	0	14
	Phaeocystis globosa	2	4	0	1	2	0	9
Bacillariophyta	*Fragilariopsis cylindrus*	1	1	1	0	3	0	6
	Phaeodactylum tricornutum	1	1	1	1	1	0	5
	Pseudo-nitzschia multiseries	2	1	1	1	1	0	6
	Thalassiosira pseudonana	1	1	1	1	0	1	5
Ochrophyta	*Ectocarpus siliculosus*	1	1	1	0	1	1	5
	Nannochloropsis oceanica	3	1	1	1	0	0	6
	Ochromonadaceae sp.	1	2	0	0	2	2	7
Chlorarachniophyta	*Bigelowiella natans*	0	2	1	1	3	0	7

27
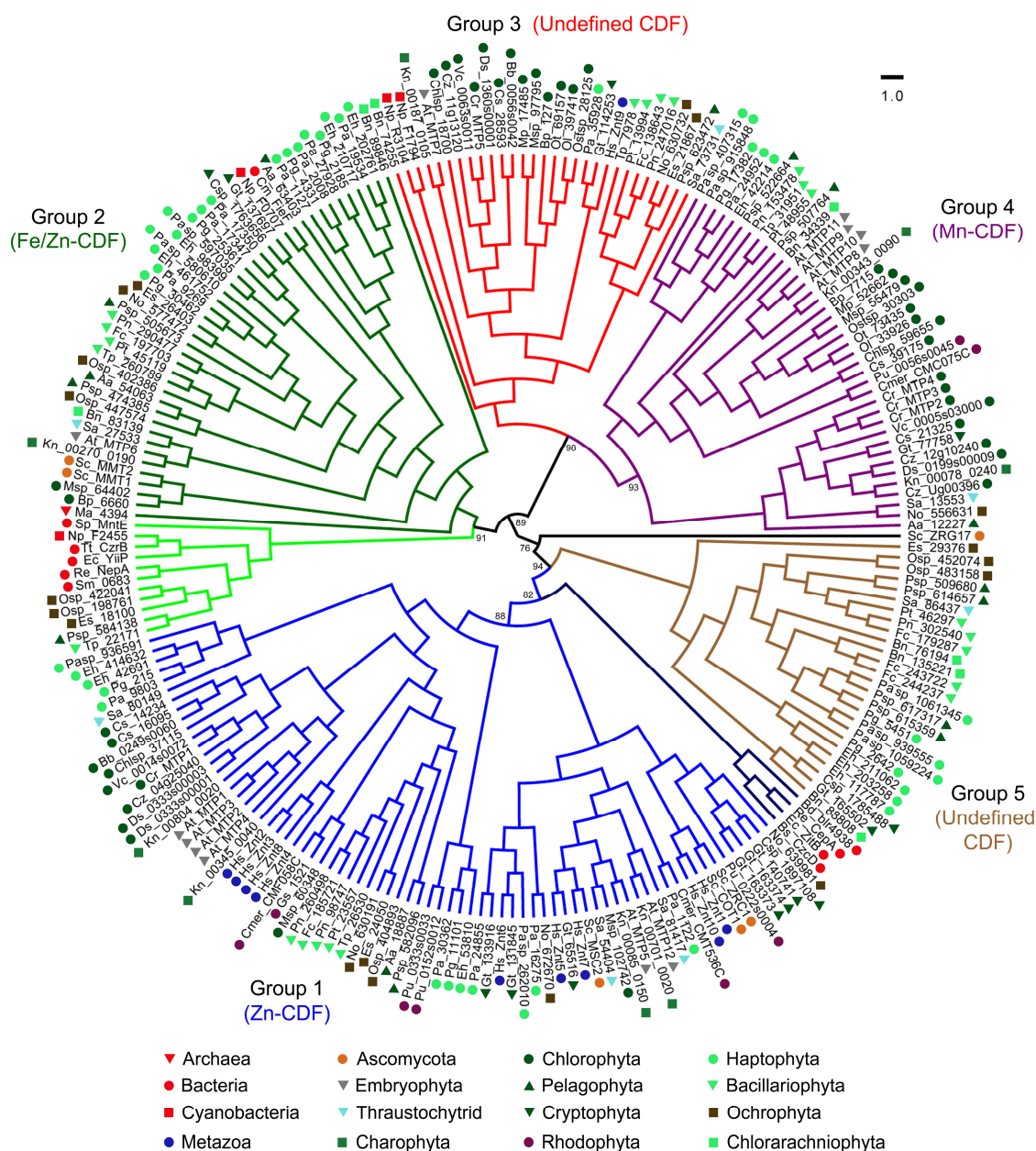
Figures

Figure 1. Phylogenetic analysis of CDF transporter family proteins from various selected algal taxa in comparison to prokaryotic, animal (*H. sapiens*), land plant (*A. thaliana*) and yeast (*S. cerevisiae*) proteins. The genome identifier or accession numbers of all sequences used are provided in Table S1. Coloured symbols indicate the major taxonomic domains of the species where the protein sequence is derived. Five major groups are highlighted. The tree was constructed using the maximum likelihood method and derived from alignments of full length amino acid sequence. A consensus tree following 1000 bootstrap replications is shown, with bootstrap percentage values indicated at the nodes of major branches. The branch length scale bar indicates the evolutionary distance of one amino acid substitution per site.

28
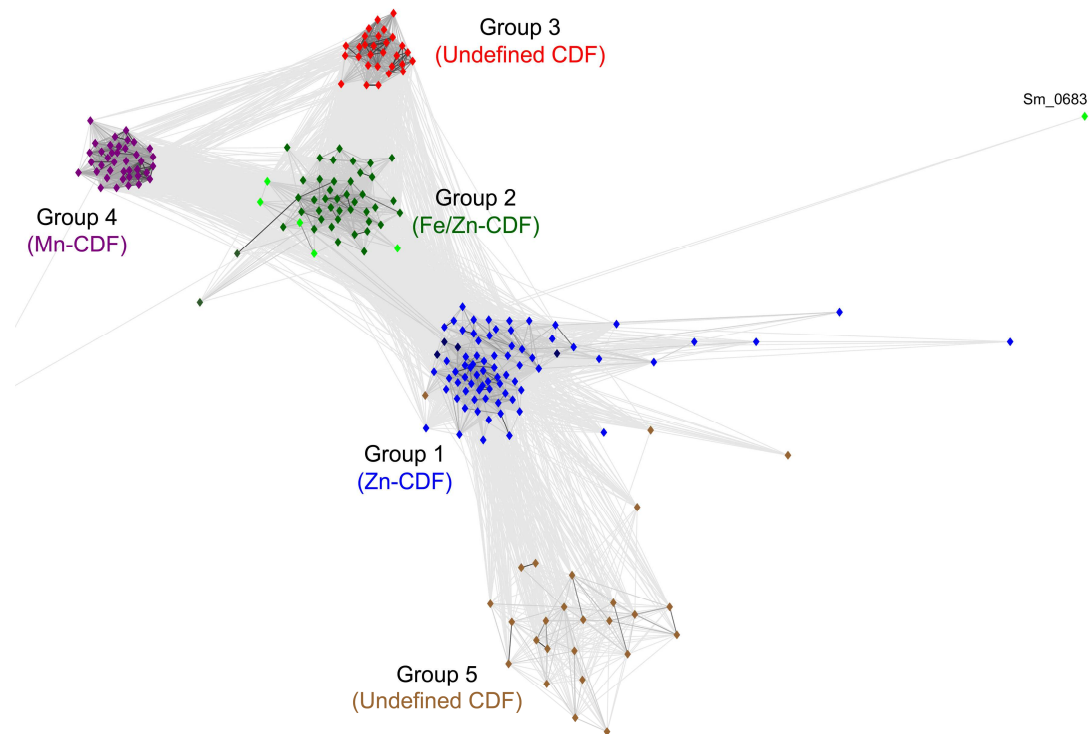
Figure 2. A two-dimensional cluster analysis of sequences representing the phenetic sequence relationship of CDF transporter family proteins from various selected algal taxa in comparison to prokaryotic, animal (*H. sapiens*), land plant (*A. thaliana*) and yeast (*S. cerevisiae*) proteins. Each symbol represents a full length amino acid sequence of an individual CDF protein and is coloured on the basis of the phylogenetic groups shown in Figure 1. Grey lines represent protein connections with reciprocal BLAST hits at $P < 10^{-5}$. Six proteins are not shown (five Group 2 members: Psp_584138, Tp_22171, Es_18100, Osp_198761, Osp_422041, and unassigned ScZRG17) as they did not cluster with any of the other sequences and are on the periphery of the plot off the scale.

29
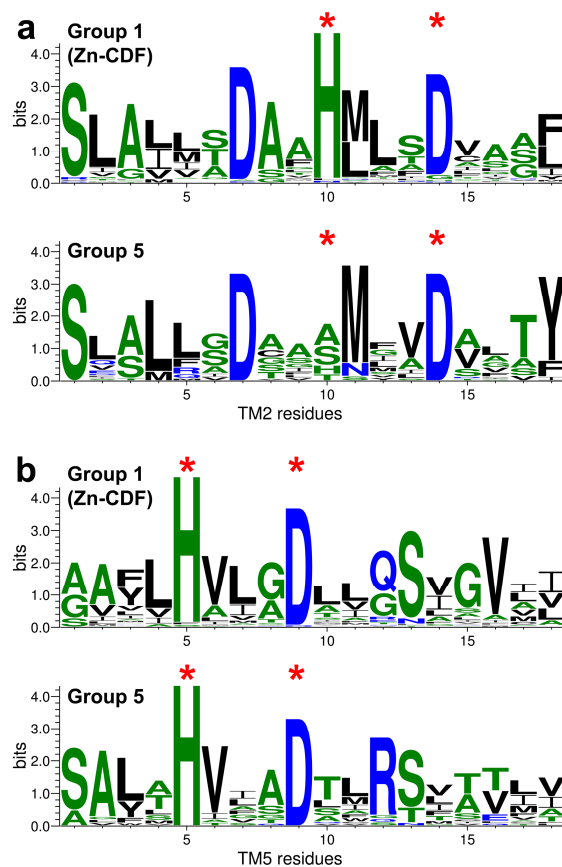
Figure 3. Comparison of conserved CDF residues within transmembrane (TM) domain 2 (a) and TM domain 5 (b) for Group 1 (Zn-CDF) and Group 5 proteins. Sequence logo representations of 18 residues within each TM domain determined for all of the Group 1 sequences and all of the Group 5 sequences. Asterisks indicate the positions of conserved active site 'A' residues.
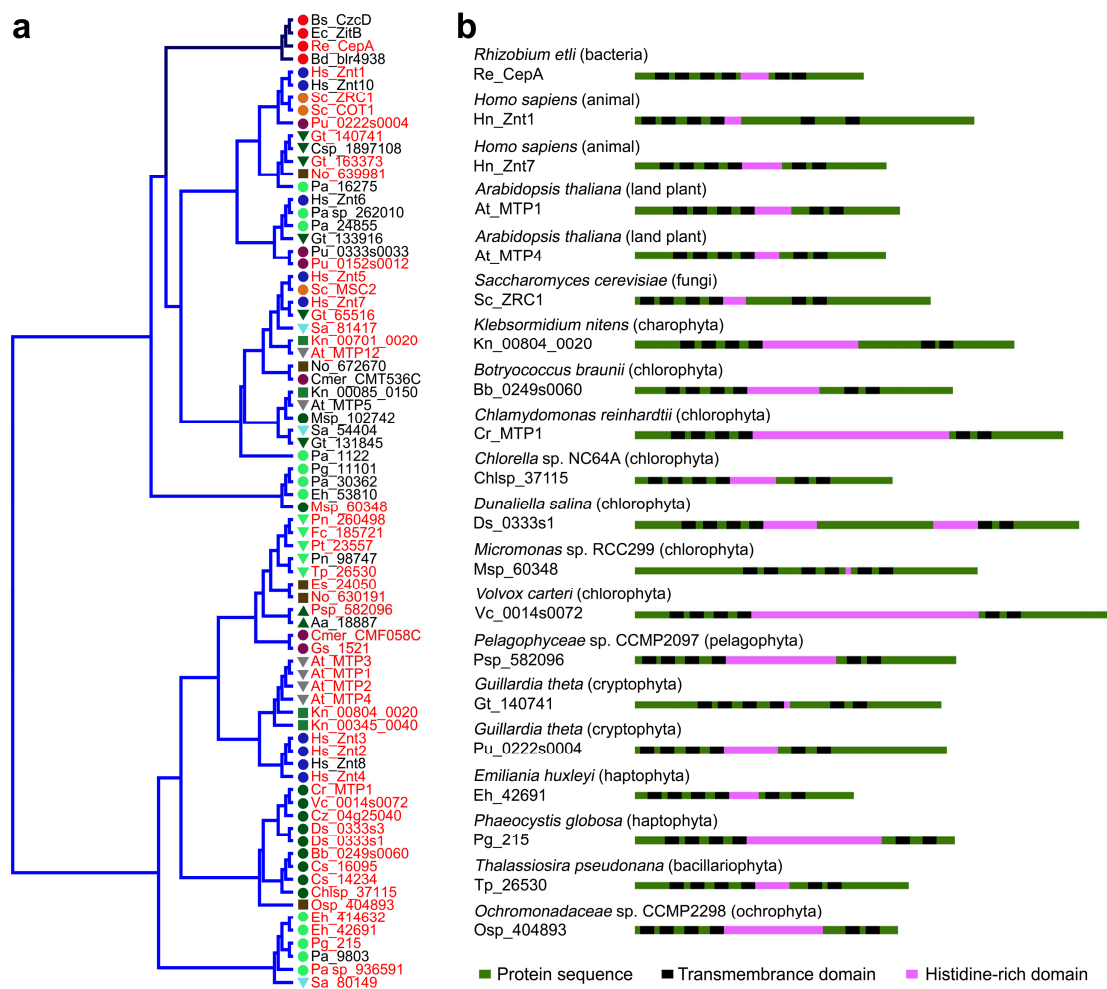
Figure 4. Analysis of Group 1 Zn-CDF proteins. (a) Phylogenetic analysis of Zn-CDF family proteins from various selected species. The coloured symbols indicating the major taxonomic domains of each species are as defined in Figure 1. Proteins highlighted in red possess an obvious histidine-rich domain. (b) Topology models of selected Group 1 Zn-CDF proteins indicating the predicted transmembrane (TM) spans and the histidine-rich domain within the major cytosolic loop between TM4 and TM5.
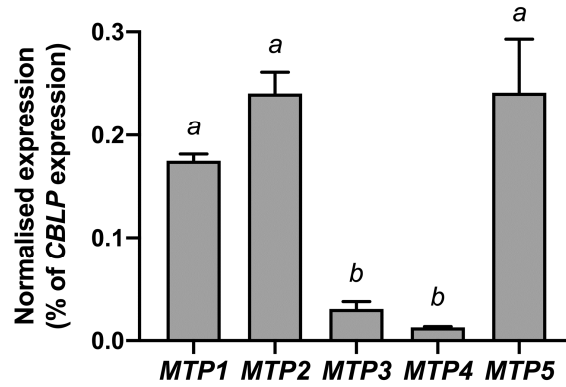
31

Figure 5. Expression the CrMTP family genes in *C. reinhardtii* cells grown in standard TAP medium at exponential growth stage. Expression of the selected mRNA transcripts as determined by real-time PCR was calculated as a percentage of *CBLP* expression. Data points are means (±SEM) calculated from biological triplicates. Bars sharing the same lowercase letter indicate no significant difference between treatments ($P > 0.05$) as determined by one-way ANOVA and Tukey post-hoc test.
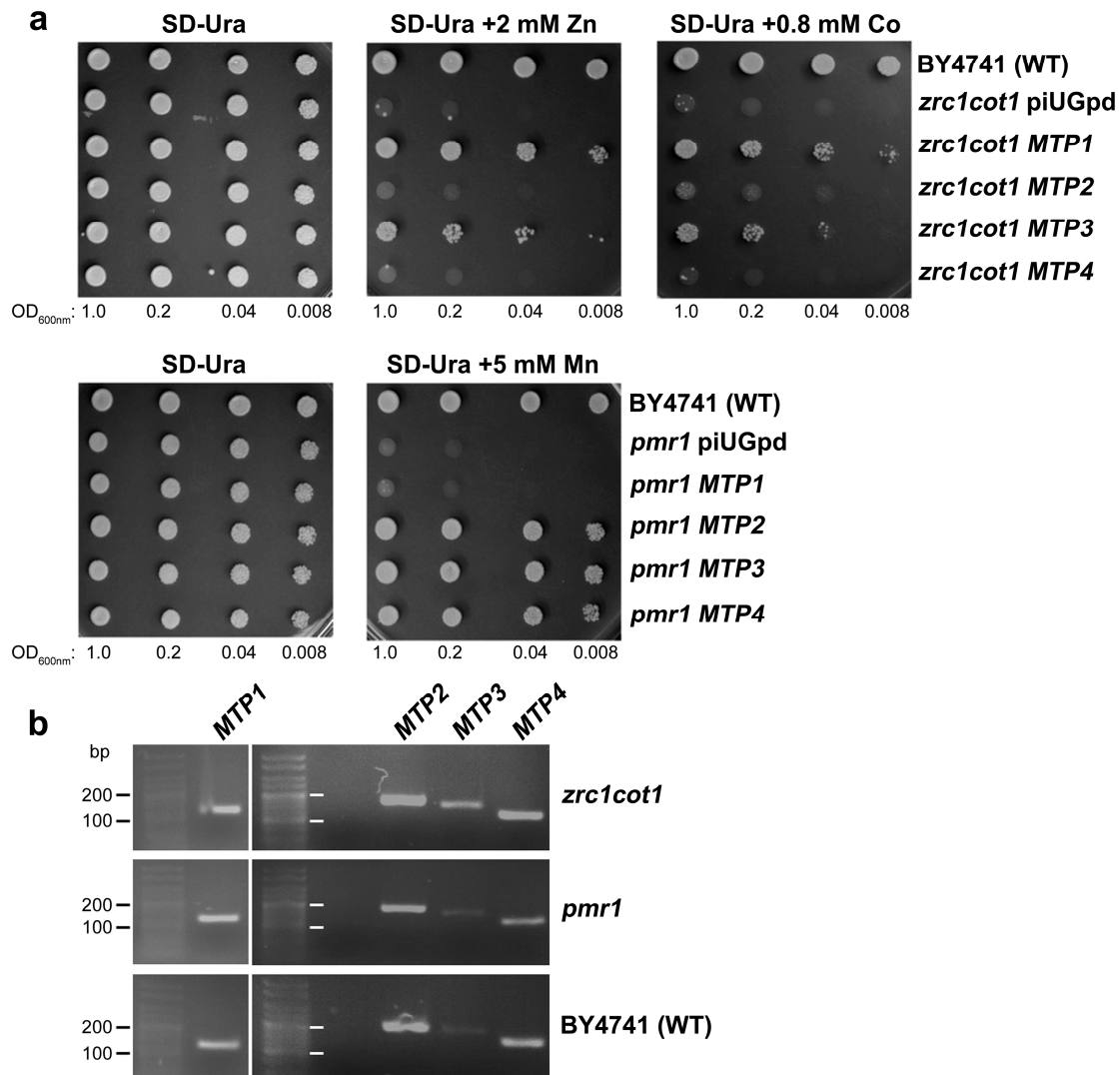
Figure 6. Heterologous expression of *CrMTP1*, *CrMTP2*, *CrMTP3* and *CrMTP4* in yeast strains. (a) Suppression of Zn, Co and Mn hypersensitivity of the Zn- and Co-sensitive *zrc1cot1* yeast mutant and the Mn-sensitive *pmr1* mutant by heterologous expression of *CrMTP* cDNA in comparison with empty vector (piUGpd) and WT (BY4741). Saturated liquid cultures of yeast strains were serially diluted to the indicated cell densities then spotted onto SD –Ura selection medium with or without added Zn, Co or Mn. Yeast growth is shown after 3 d. A representative experiment is shown. (b) RT-PCR of *MTP1*, *MTP2*, *MTP3* and *MTP4* expression in each yeast strain.
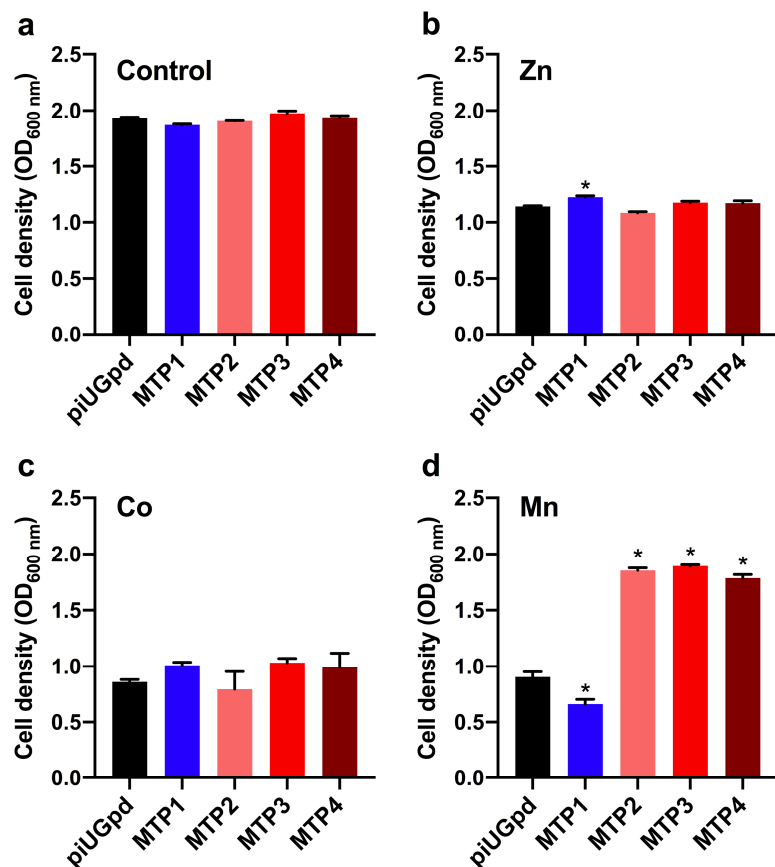
Figure 7. Heterologous expression of *CrMTP1*, *CrMTP2*, *CrMTP3* and *CrMTP4* in wild type (BY4741) yeast. Cell density measurement of strains expressing each MTP cDNA in comparison with empty vector (piUGpd) grown after 3 d in liquid SD –Ura medium either without metal exposure (a) or with 10 mM Zn (b), 10 mM Co (c), or 20 mM Mn (d). Data points are means (±SEM) from triplicate samples. Bars with an asterisk indicate significant difference between the empty vector control (piUGpd) strain ($P < 0.05$) as determined by one-way ANOVA and Tukey post-hoc test.
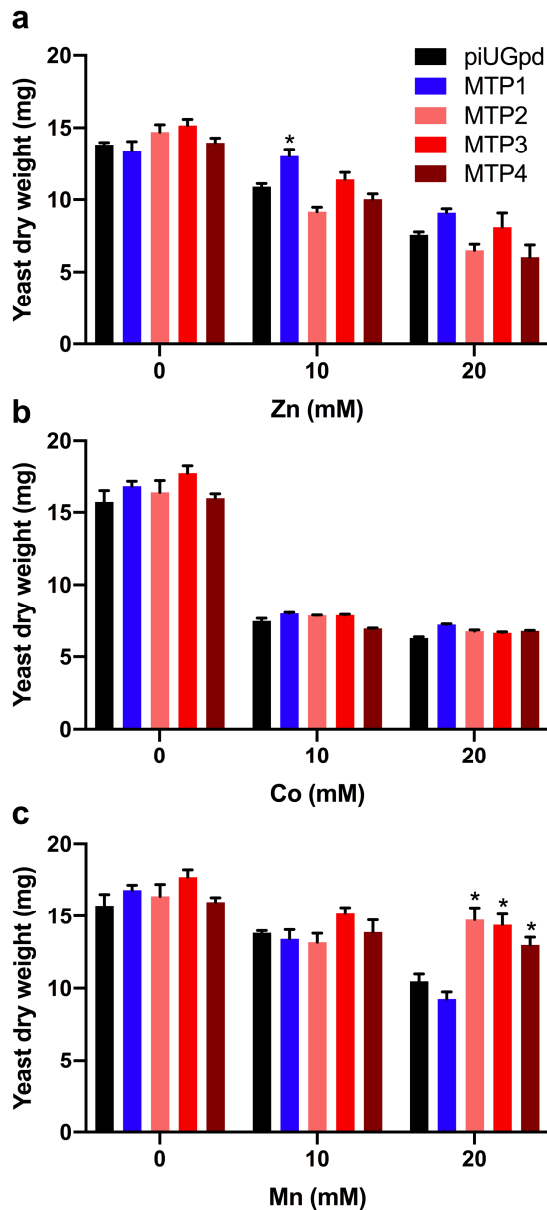
Figure 8. Heterologous expression of *CrMTP1*, *CrMTP2*, *CrMTP3* and *CrMTP4* in wild type (BY4741) yeast. Dry weight biomass measurement of strains expressing each *CrMTP* cDNA in comparison with empty vector (piUGpd) grown after 3 d in liquid SD –Ura medium either without metal exposure or with added Zn (a), Co (b), or Mn (c). Data points are means (±SEM) from triplicate samples. Bars with an asterisk indicate significant difference between the empty vector control (piUGpd) strain ($P < 0.05$) as determined by one-way ANOVA and Tukey post-hoc test.
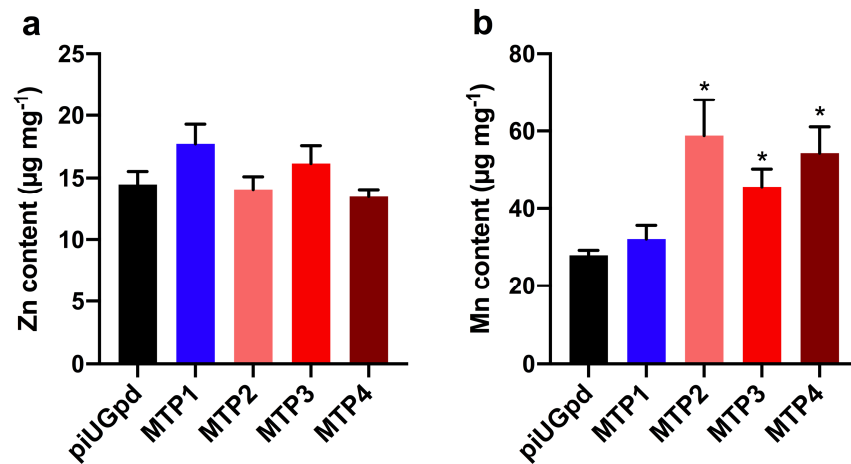
Figure 9. Zn and Mn uptake into wild type (BY4741) yeast expressing *CrMTP1*, *CrMTP2*, *CrMTP3* and *CrMTP4*. Metal content measurement of strains expressing each *CrMTP* cDNA in comparison with empty vector (piUGpd) grown after 3 d in liquid SD –Ura medium with added 20 mM Zn (a) or 20 mM Mn (b). Data points are means (±SEM) from triplicate samples. Bars with an asterisk indicate significant difference between the empty vector control (piUGpd) strain (P < 0.05) as determined by one-way ANOVA and Tukey post-hoc test.

36